LASER INTERFEROMETER GRAVITATIONAL WAVE OBSERVATORY
- LIGO -
==========
LIGO SCIENTIFIC COLLABORATION

Technical Note	**LIGO-T1400513-v1-**	2014/10/19

Measuring the Quality Factor of Cryogenic Silicon

Marie Lu, Nic Smith, Rana Adhikari, Zach Korth

California Institute of Technology
LIGO Project, MS 18-34
Pasadena, CA 91125
Phone (626) 395-2129
Fax (626) 304-9834
E-mail: info@ligo.caltech.edu

Massachusetts Institute of Technology
LIGO Project, Room NW22-295
Cambridge, MA 02139
Phone (617) 253-4824
Fax (617) 253-7014
E-mail: info@ligo.mit.edu

LIGO Hanford Observatory
Route 10, Mile Marker 2
Richland, WA 99352
Phone (509) 372-8106
Fax (509) 372-8137
E-mail: info@ligo.caltech.edu

LIGO Livingston Observatory
19100 LIGO Lane
Livingston, LA 70754
Phone (225) 686-3100
Fax (225) 686-7189
E-mail: info@ligo.caltech.edu

http://www.ligo.org/

Contents

Abstract

Cryogenic silicon is being considered as an alternate material to the current material, silica, for the test masses in future iterations of LIGO due to its potential to reduce thermal noise. For example, the thermal expansion coefficient goes to zero at 120 K. The Fluctuation Dissipation Theorem relates the amount of noise produced by a system with the system's linear response to applied perturbations. We apply this theorem to cryogenic silicon by measuring the quality factor, Q, to observe the damping behavior. This project develops a system to measure Q and study its response to frequency, drive amplitude, and temperature, and thin film depositions.

Introduction

Originally proposed in 1916 as a part of the theory of general relativity, gravitational waves and their detection have been a major investment for many scientists. LIGO, the Laser Interfermeter Gravitational-Wave Observatory, measures ripples in the force of gravity emitted from major cosmic events. The LIGO detector is a Michelson interferometer, composed of a series of fixed silica mirrors suspended from fibers in a pendulum. Because gravitational waves are incredibly weak, it is necessary to reduce noise sources as much as possible in order to obtain accurate results. Currently, the material for the wires–fused silica– still contributes significant thermal noise uniformly across the noise floor, preventing the detectors from reaching their quantum mechanical sensitivity limits. Our research will focus an alternative material, silicon, for the fibers that has lower thermal fluctuations. This material will likely operate under cryogenic temperatures to minimize the mechanical dissipation of atoms vibrating from thermal fluctuations.

In reality, thermal fluctuations are incredibly small and hard to measure accurately. So instead, the fluctuation dissipation theorem allows us to measure the mechanical dissipation of a material, which is directly related to the amount of thermal fluctuations. To derive one from the other, we start with the equation of motion of the particles inside a material modeled by

$$\ddot{x} = -\omega_0^2(1 + i\phi)x + F \tag{1}$$

where ϕ is the loss angle for Zener (thermoelastic) damping:

$$\phi = \Delta \frac{\omega\tau}{1 + \omega^2\tau^2} \tag{2}$$

Although other forms of damping exist, we expect to be limited by Zener damping. We define

$$\Delta \equiv \frac{\alpha^2 Y T}{\rho C_p} \tag{3}$$

α is the coefficient of thermal expansion, Y is Young's Modulus, T is the temperature, ρ is the density, and C_p is the specific heat capacity.

In addition,

$$\tau \equiv \frac{\rho C_p t^2}{\pi \kappa} \tag{4}$$

with thickness, t.

Another parameterization of the equation of motion can be obtained by replacing the complex component with a variable γ, resulting in

$$\ddot{x} = -\omega_0^2 x - \gamma \dot{x} + F \tag{5}$$

where $\gamma = \frac{\omega_0^2 \phi}{\omega}$, which we find from setting the two differnt paratmeterizations equal to each other. This results in the the power spectrum of the motion of the mass

$$x^2(\omega) = \frac{4k_B T \sigma(\omega)}{\omega^2} \tag{6}$$

with $\sigma(\omega)$ denoting the mechanical conductance, which is also the real part of the admittance:

$$Y(\omega) = \frac{\omega\phi + i(\omega - m\omega^3)}{(k - m\omega^2)^2 + k^2\phi^2} \tag{7}$$

Solving for $\sigma(\omega)$ and substituting into Equation 6 produces the power spectral density of the position of the mass:

$$x^2(\omega) = \frac{4k_B T k \phi(\omega)}{\omega[(k - m\omega^2)^2 + k^2\phi^2]} \tag{8}$$

Thus, in order to map out the noise spectrum, our experiments measure ϕ, a quantity that is inversely proportional to the quality factor of the material, as we will show later.

Methods of Determining the Quality Factor

The first method is the ringdown technique, which consists of driving the cantilever at resonance, removing the driving force, and recording the exponentially damped oscillations. If we start at the equation of motion (Equation 5) and solve for the transfer function, we see that the quality factor is directly proportional to the time constant. Setting $\overline{x}$ and $\overline{F}$ as the Laplace transforms of x and F, respectively, we take the Laplace transform of both sides of our equation of motion, giving

$$s^2\overline{x} = -\omega_0^2\overline{x} - \gamma s\overline{x} + \overline{F} \tag{9}$$

Solving for $\frac{\overline{x}}{\overline{F}}$ produces the transfer function:

$$\begin{aligned}\frac{\overline{x}}{\overline{F}} &= \frac{1}{s^2+\gamma s+\omega_0^2} \\ &= \frac{1}{(s+\frac{\gamma}{2})^2+(\omega_0^2-\frac{\gamma^2}{4})} \\ &= \frac{\sqrt{\omega_0^2-\frac{\gamma^2}{4}}}{(s+\frac{\gamma}{2})^2+(\omega_0^2-\frac{\gamma^2}{4})}\frac{1}{\sqrt{\omega_0^2-\frac{\gamma^2}{4}}}\end{aligned}$$

Now we take the inverse Laplace transformation to obtain the impulse function:

$$I(t) = e^{-\frac{\gamma}{2}t}\sin\sqrt{\omega_0^2-\frac{\gamma^2}{4}}t \tag{10}$$

We may make the approximation that $\frac{\gamma}{\omega_0}$ is small, making $\frac{\gamma^2}{4}$ is negligible compared to ω_0^2:

$$I(t) = e^{-\frac{\gamma}{2}t}\sin\omega_0 t \tag{11}$$

This is a damped sinusoid with a time constant $\tau = \frac{2}{\gamma} = \frac{2\omega}{\omega_0^2\phi}$

By definition, the quality factor is

$$Q \equiv \frac{\omega_0}{\Delta\omega} \tag{12}$$

where $\Delta\omega$ is the bandwidth, or, the full width at half max of the peak centered at the resonant frequency of the transfer function. Because τ is the time it takes for the wave to decay to $\frac{1}{e}$ of the original power, in frequency space we can observe that $2\frac{1}{\tau} = \Delta\omega$ so then $Q = \frac{\omega_0\tau}{2}$. Thus from the ringdown experiment, we can obtain τ and thus Q.

Furthermore, if we substitute $\tau = \frac{2\omega}{\omega_0^2\phi}$ into $Q = \frac{\omega_0\tau}{2}$, then

$$Q = \frac{1}{\phi} \tag{13}$$

with the substituion of $\omega = \omega_0$, because the quality factor is only defined at the peak of the resonant frequency. Thus by measuring the time constant from the decaying sinusoid of the cantilever, we can find the quality factor and the needed value of ϕ for the noise spectrum (Equation 8).

The second method is to drive the oscillator with white noise and to study the cantilever's transfer function. Again, from the definition of $Q = \frac{\omega_0}{\Delta\omega}$, we can look at the transfer function of the cantilever's motion and fit a Lorentzian curve to the peak at the resonant frequency, thus obtaining the value of the resonant frequency and the bandwidth to calculate Q and ϕ.

However both of these experiments have impracticalities in exectuion. The first method is applied with the assumption that the driving frequency is exactly at the resonant frequency

with an accuracy of at least one part in Q. This can be difficult in practice. In addition, the ringdown time in the first method can be several hours, presenting another practical concern. Lastly, we assumed in both of the previous methods that the measurement of Q is independent of the driving amplitude. However, a greater drive may increase the friction within the clamp and contribute complicated damping to the system that will confuse our measurements of Q.

This final method, which is still in the process of being implemented, addresses these issues. This design (See Figure 6) uses two control loops to keep the driving force locked to the natural resonant frequency and to lock the oscillator at a fixed oscillation amplitude. The phase locked loop (PLL) is achieved by making the auxiliary oscillator a voltage controlled oscillator (VCO) that is locked to the signal of the position output. The amplitude locked loops is comprised of an amplitude detector which is then compared to a reference amplitude. The error signal is amplified and used to adjust the strength of the drive.

To see how this method measures the quality factor, we will focus on the output of the amplitude control output and the amplitude amplitude set point, which we will call a and c respectively. We will also do our analysis referring to the linearized model of the ALL (Refer to Figure 7). Then,

$$\frac{a}{c} = \frac{H}{1+G} \tag{14}$$

$$= \frac{H\phi\omega_0(1+i\tau\omega)}{(\phi\omega_0 + \frac{SHA}{\omega_0})(1+\frac{2i\omega}{\phi\omega_0}+\frac{SHA}{\omega_0})} \tag{15}$$

If we take the limit of high gain and solve for ϕ, we arrive at

$$Q = \phi^{-1} = (\frac{2\omega_U}{cH_U\omega_0}\langle a\rangle)^{-1}. \tag{16}$$

where $\omega_U = \frac{|SH_UA|}{2\omega_0}$ is the unity gain frequency and H_U is the gain of H at the unity gain frequency.

With this implementation, Q is can be calculated continuously and instantaneously from the information used to maintain the control loops, which is an advantage over the ringdown technique, which may take up to several hours to complete. In addition, all of the Q measurements from this process are made at a constant, chosen amplitude. Thus, we can control the amplitude to determine how Q depends on drive amplitude, possibly giving indications on the amount of clamp loss present. This could be useful if we wish to improve the clamp design in the future.

Clamp Models

Before we make any measurements of the thermal dissipation of our silicon wafer, we must design an experimental set-up. In particular, we need to find a clamp structure to hold the silicon test mass that minimizes the amount of clamping loss. The goal of our experiment is to measure damping. If the clamp is introducing damping external to the inherent damping

of the silicon, then our measurements will be affected. This phemonenon is described by

$$\phi_{measured} \approx \phi_{Si} + R\phi_{clamp} \tag{17}$$

where $R = \frac{E_{clamp}}{E_{clamp}+E_{Si}}$. E_{clamp} and E_{Si} represent the strain energy in the clamp and silicon test mass, respectively. The strain energy is the a measurement of the amount of energy stored in a system due to deformations. Ideally, we would like to minimize R such that our measurements mainly reflect the loss in the silicon.

The silicon cantilevers are etched out of whole silicon wafer (See Fig 1 for reference). The clamp will hold the wafer on either side, at the center, secured by a screw that will pass through the center hole. Initially, we hypothesized that reducing the area of contact between the silicon wafer and the steel clamp components would lessen the clamp loss. Thus we played with model shapes that would test this factor.

Here are the three major clamp designs that we focused on:

- Model 1: The clamp is composed of two solid cylinders on either side of the wafer held in place by a screw.
- Model 2: Two cylindrical disks, one on either side of the wafer, are supported on four hemispheres, making contact with the silicon surface at only four points on each side of the wafer. The four contact points form a square.
- Model 3: Two solid cylinders, one on either side of the wafer, with the center of the cylinders are hollowed out such that there is only a ring of contact between the steel clamp and the wafer.

We found that a Model 1 clamp with a 6 mm radius produced a minimum $R \approx 10^{-3}$. Models 1 and 3 produced strain energy ratios that were 2 orders of magnitude better than that produced by Model 2. Thus we will focus on Models 1 and 3 in this discussion. Shortening the radii allowed for smaller clamp loss in both designs (Refer to Figure 4 for a plot of strain energies over the eigenfrequencies). Although Model 3 has lower strain energy ratios at eigenfrequencies below approximately 245 Hz, our experiment mainly pertains to eigenmodes of the rectangular cantilevers on the wafer, which are from 251 to 298 Hz. This is where Model 1 consistently produced lower strain energy than Model 3, although the two are close.

Designing the Experiment

Based on the constraints of the model we developed, we then drafted a experimental set-up in SolidWorks. See Figure 5 for details on the design. The silicon cantilever is excited into oscillatory motion by an electrostatic driver (ESD) and an optical lever captures the motion. A helium neon laser enters through a slit centered between the spacers holding up the ESD, bounces off of the 45 degree mirror onto the oscillating cantilever above, and back onto the mirror and out of the slit. The signal is detected by a quadrant photodiode (QPD). As the cantilever moves up and down, the angle of reflection of the beam will change, and

we observe the oscillating behavior and calculate the quality factor with the three different methods described above. There is a power resistor to control the temperature. Liquid nitrogen at the base of the assembly keeps the system cool to a minimum of 77 K. However, if we wish to raise the temperature, the power resistor provides heat. The insulating layer beneath the clamp is used to keep the heat from flowing out into the liquid nitrogen too quickly if we choose to apply heat. A small resistor placed in the groove of the bottom clamp will sense the temperature. The entire system is under vacuum.

Measurements on Aluminum

While we waited for the parts of our experimental setup to arrive from the machine shop, we made practice measurements of Q on aluminum sham cantilevers using the old experimental design. All of our measurements were made with the ringdown method described above.(See Table 1 for summary of results.) With the timestream data from the ringdown method, we extracted the peak points of the decaying wave with a Python function that identifies local extrema and curve fitted the points to

$$y = Ae^{-Bt} + C \tag{18}$$

Using this technique, we found an average Q of 363 ± 1.

For the transfer function method, we fitted a Lorentzian with a linear term to the Laplace transform of the timestream data:

$$y = \frac{A}{B^2 + (x - \omega_0)^2} + mx + C \tag{19}$$

By definition, $x = (\omega_0 \pm \frac{1}{2}B)$ is the position of the half maximum. Thus from our curve fit, we obtained $\Delta\omega$ and ω_0, allowing us to calculate Q. We believe there is a linear term in our data due to noise possibly. However, the level is so very low ($m \approx 1 \times 10^4$) and is not a large source of error in meausring Q.

We found that the Q was 246 ± 4.92. See Figures 8 and 9 for examples of our fits. For each of our tests, we found the error by using the covariance matrix produced by the Python curvefit function and error propagation:

$$s_Q^2 = \sum_{i=1}^{N} (\frac{\partial A}{\partial x_i})^2 s_{x_i}^2 \tag{20}$$

and N is the number of variables that Q depends on, s_Q is the standard deviation of Q, and s_{x_i} is the standard deviation of each variable x_i. While this old set up does not give an accurate Q value due to high clamp losses, we do see consistency with among the results which indicates that our theory has good backup, but that we are limited by systematic issues that we expect our new clamp to eliminate.

Measurements on Silicon

We repeated the processes above on silicon, and measured a maximum Q of 1.05×10^4 at 77K. To make these measurements, we first injected white noise into the ESD signal to drive the cantilever and noted from the power spectrum that there are two main eigenmodes that have the highest response: at 241.5 Hz and 252 Hz. Thus we mainly drove at these frequencies for the ringdown measurements.

It is important to point out that our results differ from the expected theoretical results by at least 10^3. See Figure 10 for a comparison of our results as a function of temperature versus the theoretical predictions given by our equation (blue line)

$$\phi = \frac{1}{Q} = \Delta \frac{\omega\tau}{1+\omega^2\tau^2} \tag{21}$$

The discrepency the our expected values and and our data is most likely the result of clamp loss. Recall Equation 17. Currently we believe, $\phi_{measured}$ is dominated by the $R\phi_{clamp}$ term. Based on our simulations discussed in the section "Clamp Models" and Figure 4, we expect $R \approx 3.25 \times 10^{-3}$. Thus the quality factor of the steel clamp ($\frac{1}{\phi_{steel}}$) is on the order of magnitude of 10^{-2} to 10^{-1}, varying as a function of temperature by a exponential law:

$$Q_{steel} = [\phi_0 e^{\phi_1 \frac{T}{300}}]^{-1}, \text{ with } \phi_0 \text{ and} \phi_1 \text{ constants} \tag{22}$$

which we curve fit to our data to produce the green curve in Figure 10. Note that this is a guess we made, given the shape produced by our data. Further data collection will be needed to modify this model. By our current best fit parameters ($\phi_0 = 2.94 \times 10^{-2}, \phi_1 = 3.03$), the Q_{steel} that resulted from our experiment is about two orders of magnitude too low for steel. We believe this is a result of additional forms of loss in our clamp that are not shown through simulations and that we have yet to understand. Our simulations assume that the contact between the silicon and clamp is perfectly flat. However, in reality, there could be some curvature to the wafer or the clamp that increases the strain energy in the clamp.

Improving Clamp Loss

While clamp loss can be a function of the clamp design, it could also be dependent on the shaper of the silicon. However, simulations show that a thinner wafer, with narrower cantilevers can reduce R by another factor of 10. Using COMSOL's finite element analysis, we looked at changes in the strain energy ratio of the clamp due to one adjustment of a characteristic of the wafer at a time. See Figures 11 and 13 for the results of COMSOL simulations comparing strain energy ratios of wafers with varying thicknesses and cantilever widths, respectively. The dots indicate R for each eigenfrequency. The large peak at the beginning of each line is the eigenfrequency of the common mode motion of the pairs cantilevers. This is the mode with the most motion and is easiest to detect through our optical lever. Reducing the thickness and width of the cantilevers clearly lowers R for this peak.

Future Work

We would like to improve our clamp until we can measure a maximum Q of 10^8 or higher, and see that we can can carefully control Q with temperature, providing a sensitive and accurate measuring procedure. In addition, we will replace the ringdown method with the control loops in order to constantly measure Q. With these improvements, we will then use our system to observe changes in Q due to thin film deposition on the wafer. Mirrors made from silicon require several layers of thin film deposited on the surface to control reflectivity. Films are desposited at high temperatures and differing rates of cooling between silicon and the film material will cause stress and friction between the materials, thus changing the overal loss in the mirror.

We have been developing ways to simulate this resulting curvature using finite element analysis in COMSOL. From our simulations, we expect there to be a slight curvature in the silicon due to compressive stress in the film (Figure 14).

Figures

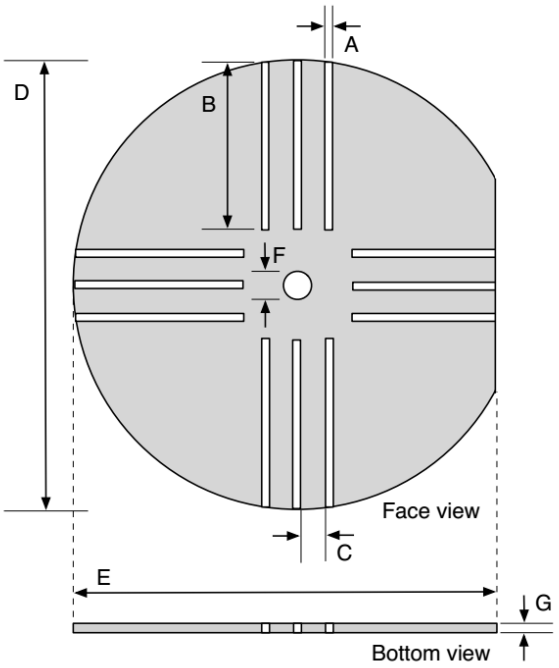

Figure 1: A = 1.5 mm, B = 34 mm, C = 10 mm, D = 100 mm (as per their info), E = (100 - X) mm, where X = flat sagitta (yet to be specified), F = 10 mm, G = 0.3 mm

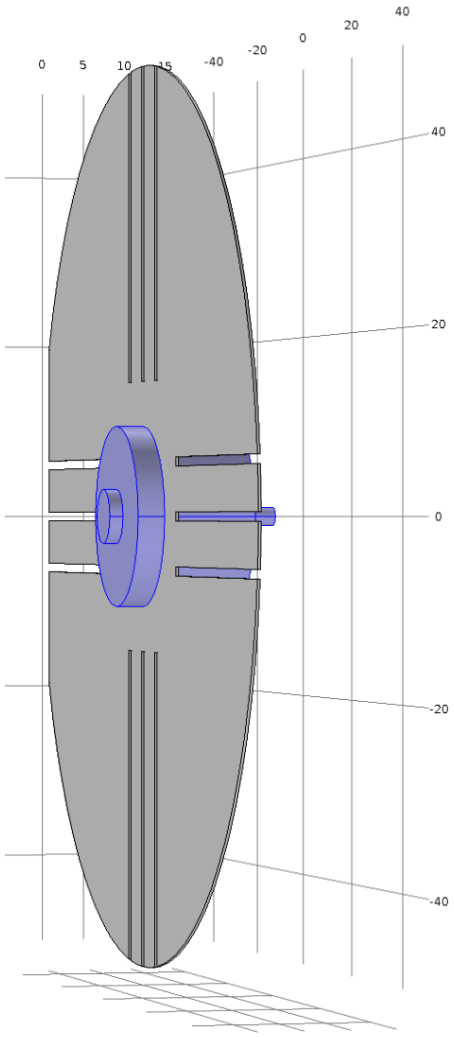

Figure 2: Model 1, front view

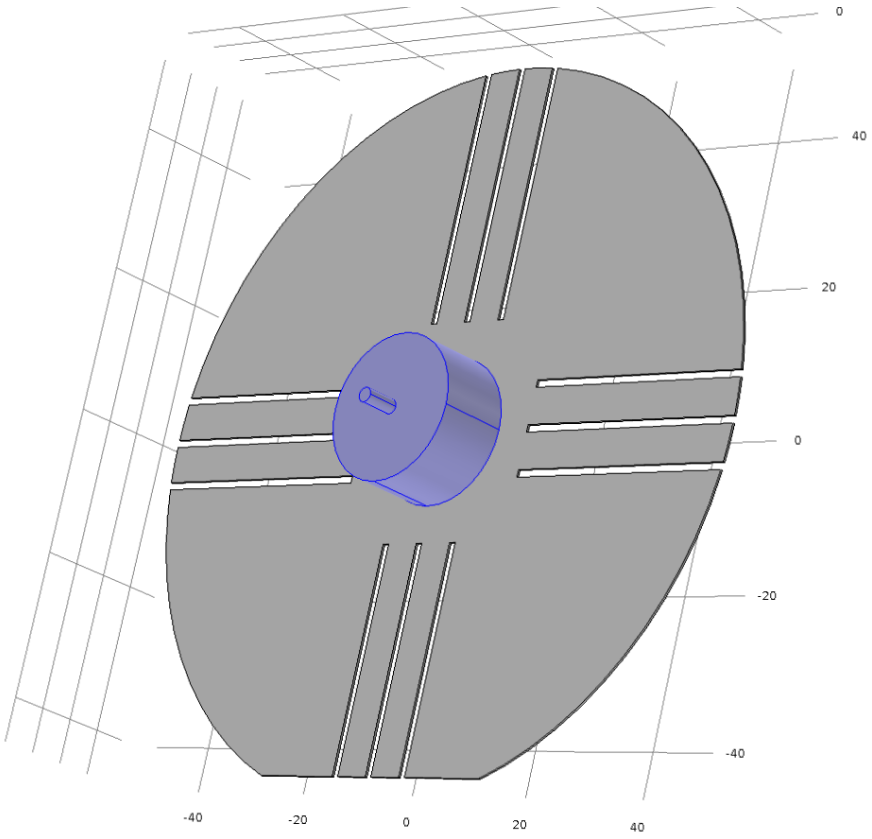

Figure 3: Model 1, back view

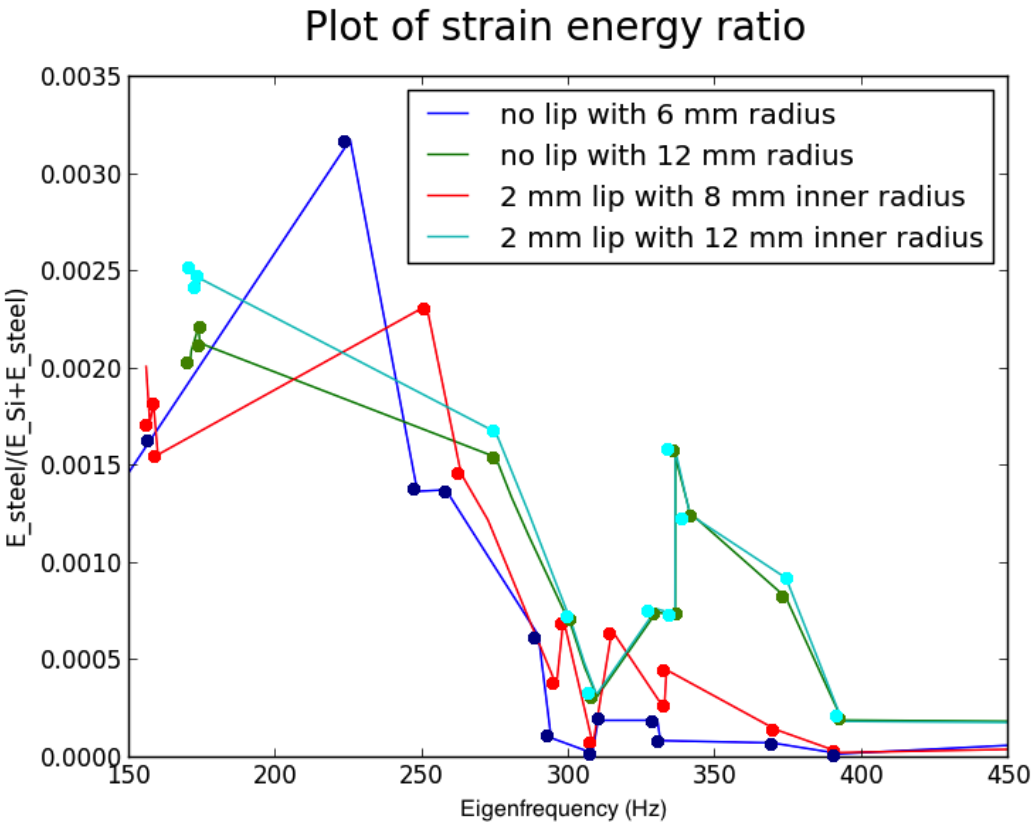

Figure 4: Comparison of strain energy ratio between Models 1 and 3 with varying radii

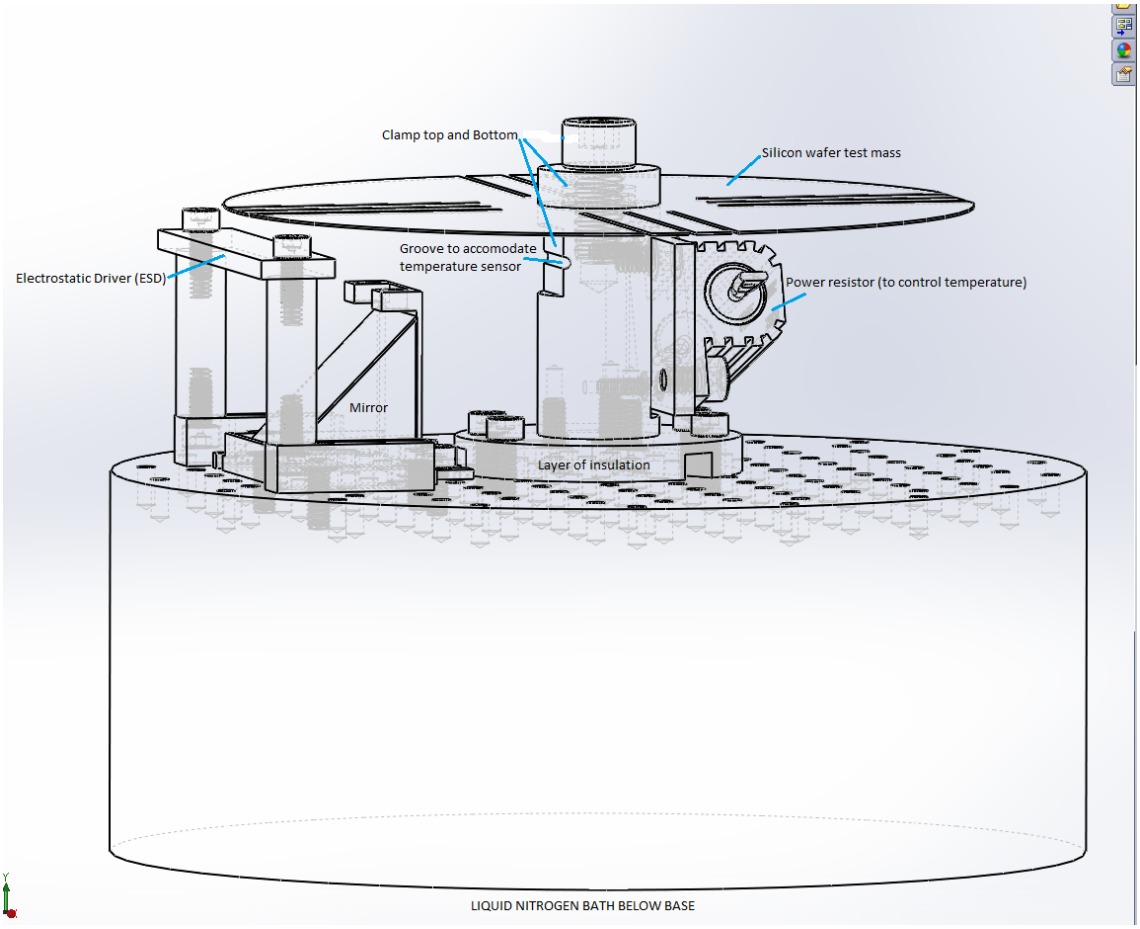

Figure 5: Experimental set-up. The ESD sends electrical pulses that will drive the thin cantilevers in the wafer. Although the base will be at liquid nitrogen temperature, we adjust the temperature of the silicon with the power resistor on the back of the bottom clamp. A laser will come in from the side, reflect off of the mirror onto the oscillating cantilever and bounce back to a quadrant photodetector

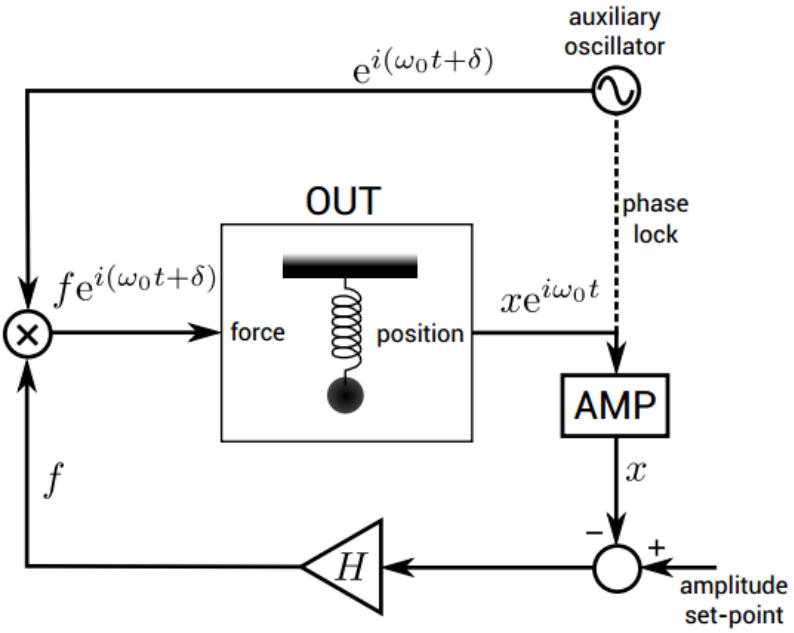

Figure 6: Block diagram of driving system. The oscillator under test (OUT) is driven by an auxiliary oscillator phase locked to the position signal. The amplitude is detected using an amplitude detector, labeled AMP. The amplitude is controlled by an amplitude locked loop (ALL).

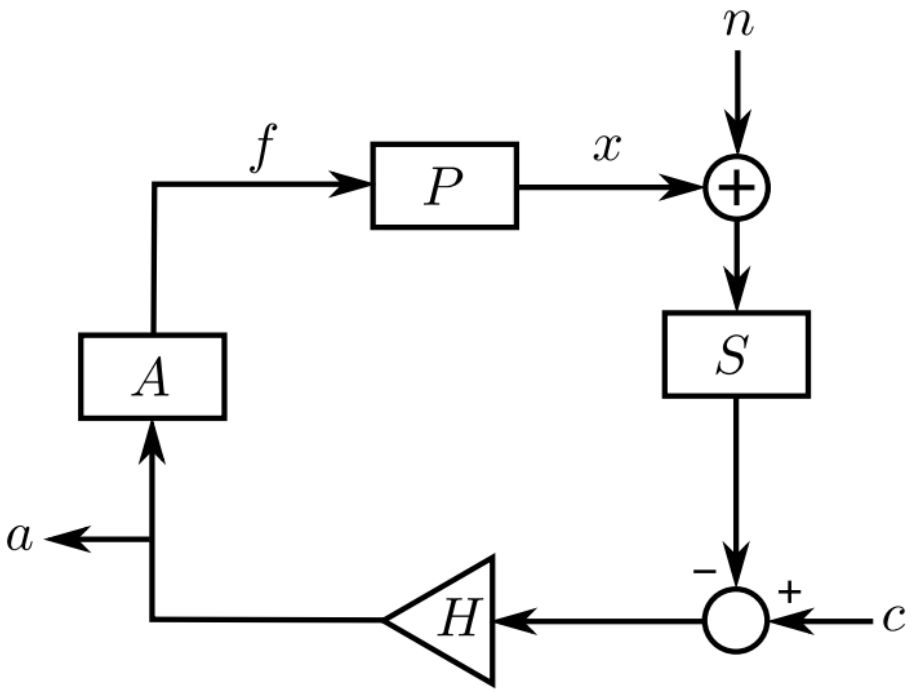

Figure 7: Linearized block diagram of the amplitude locked loop.

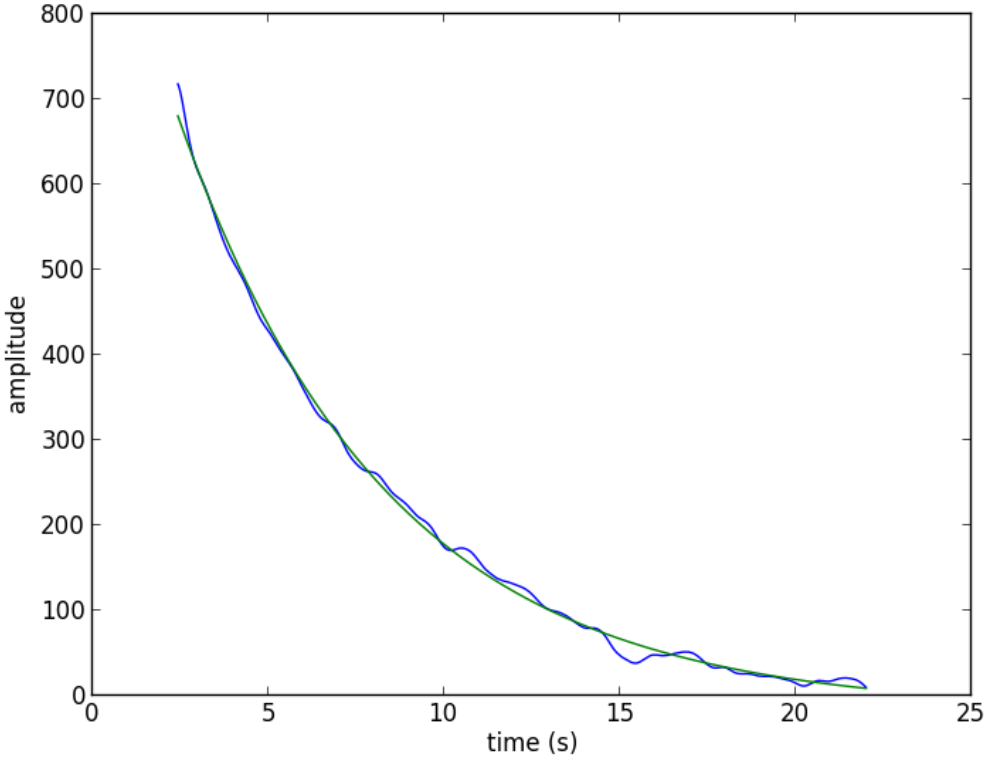

Figure 8: Green line is the curvefit of the exponential ringdown.

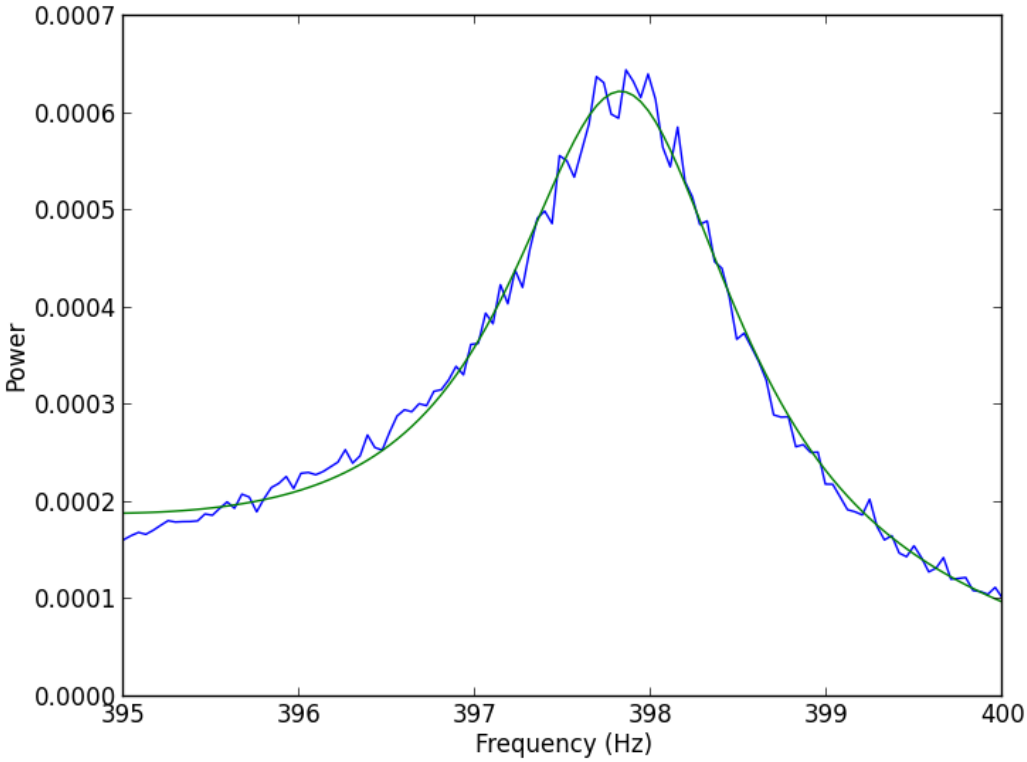

Figure 9: Green line is the curvefit of the transfer function.

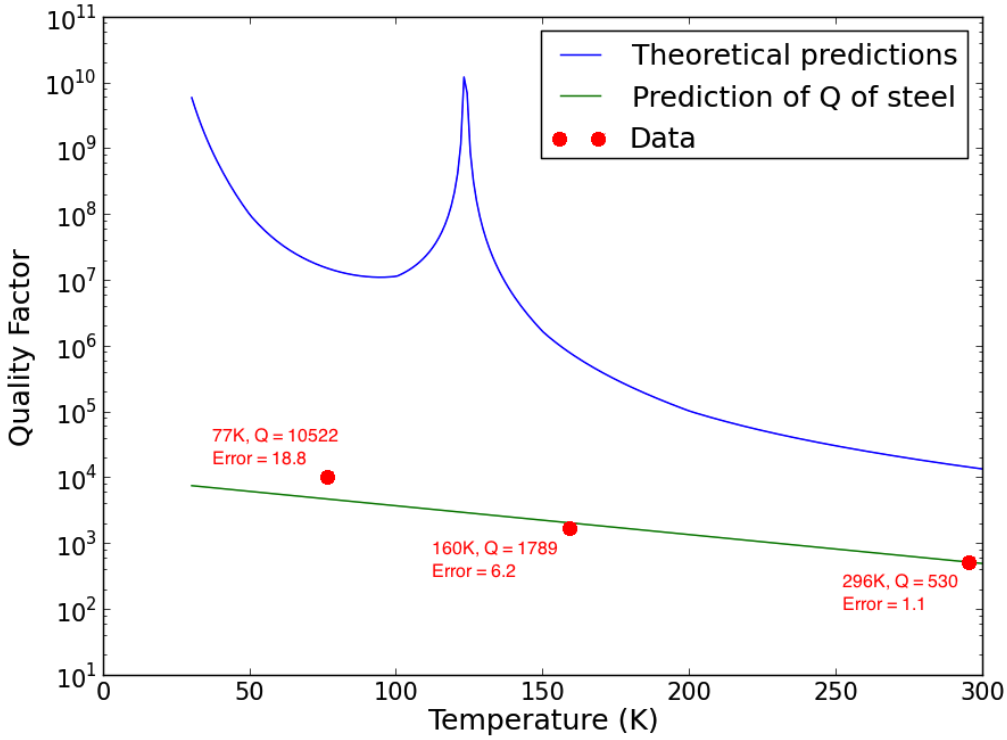

Figure 10: Comparison of theoretical predictions with our data

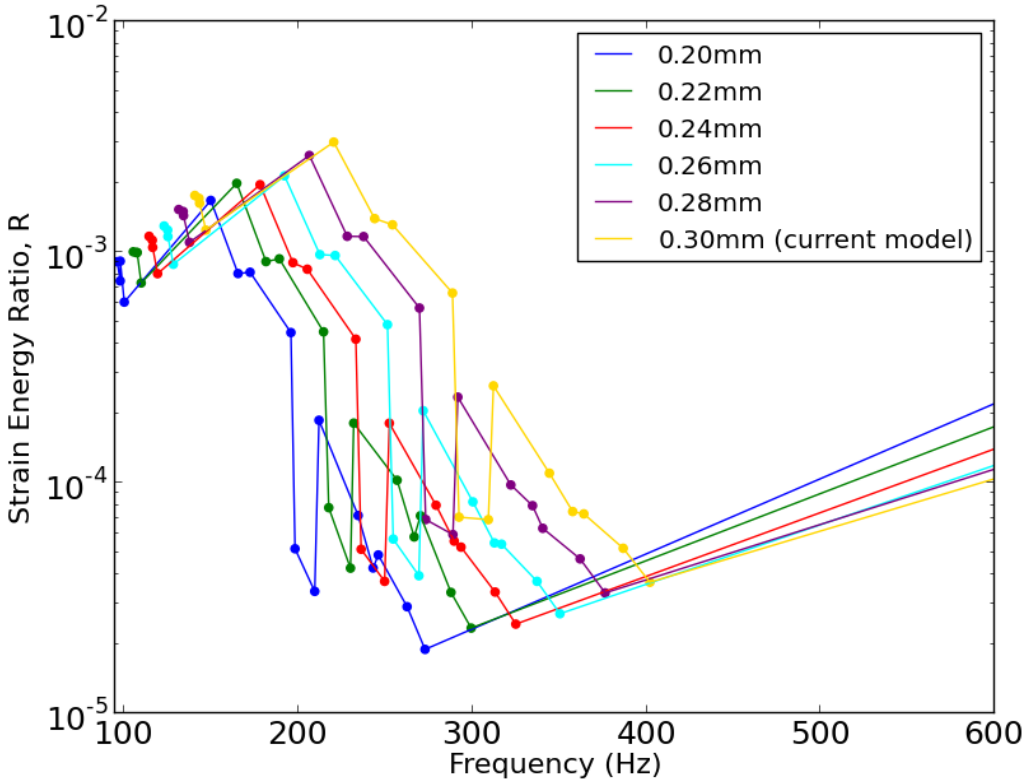

Figure 11: Reducing the thickness of the silicon will lower clamp loss

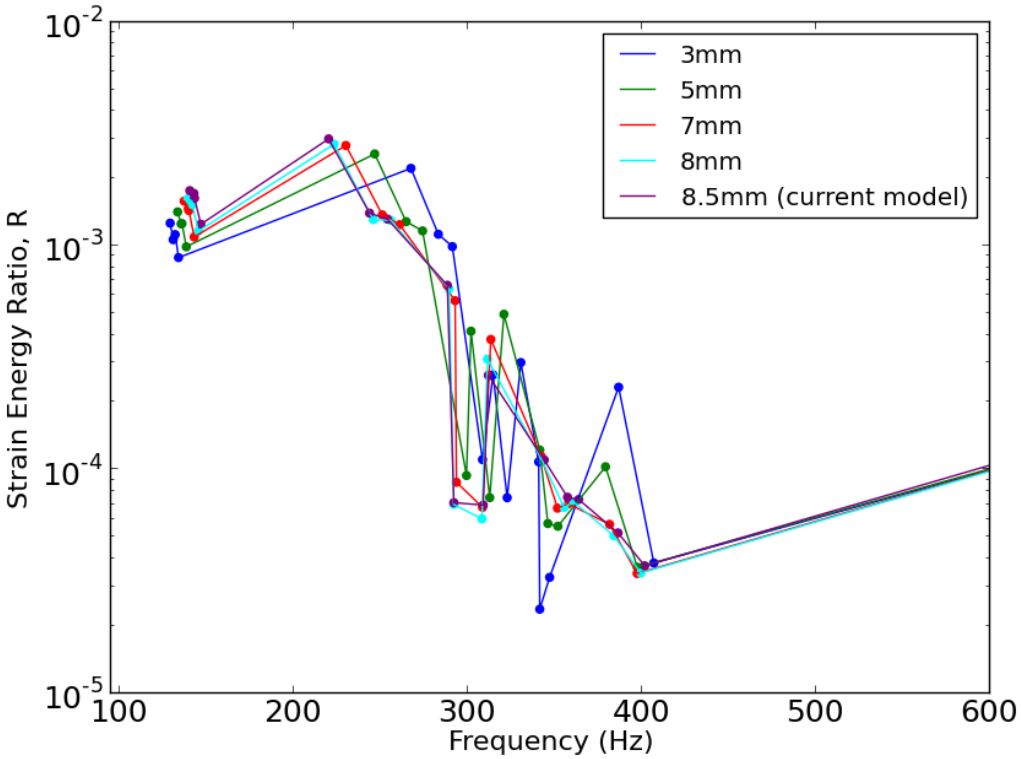

Figure 12: Reducing the width of the cantilevers will lower clamp loss

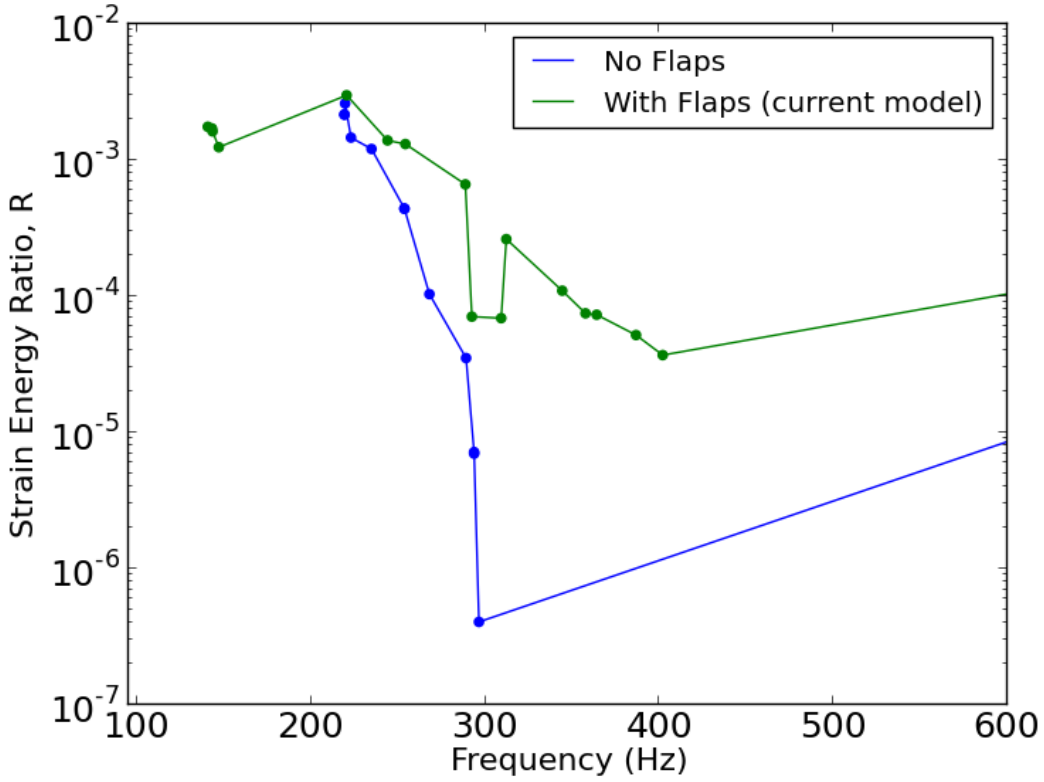

Figure 13: Removing the flaps will by reduce the clamp loss of the higher order modes.

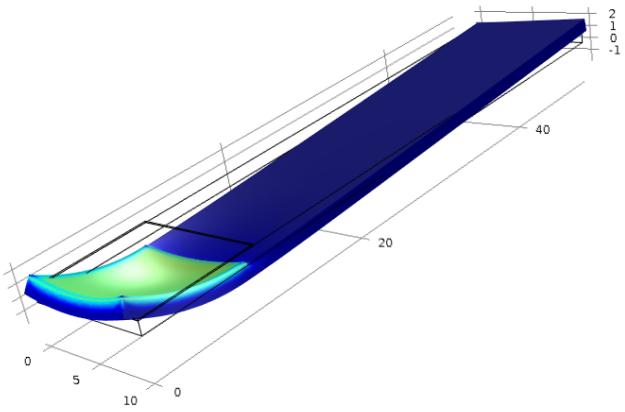

Figure 14: Example of curvature produced by a thin square of film on the tip of a silicon cantilever.

Tables

Trial #	Method	Q with error
1	Ringdown	371.0 ± 0.8
2	Ringdown	$355.4 \pm .7$
3	Transfer Function	247 ± 4.92

Table 1: Measurements of the quality factor of aluminum cantilevers.

References

[1] Nawrodt, Ronny. "Investigations of mechanical losses of thin silicon flexures at low temperatures." arXiv, 15 Mar. 2010. Web.28 Apr. 2014. http://arxiv.org/pdf/1003.2893v1.pdf.

[2] Painter, Oskar. "Laser cooling of a nanomechanical oscillator into its quantum ground state." Nature 478(): 89-92, Print.

[3] Saulson, Peter. "Thermal noise in mechanical experiments." Physical Review D42 (): 2437-2445. Print.

[4] Veggel, A A Van. "Silicon mirror suspensions for gravitational wave detectors." Classical and Quantum Gravity (): 025017. Print.

[5] Thanks to my mentors Nicolas Smith-Lefebvre, Professor Rana Adhikari, and Zach Korth for their input! I'd also like to thank Professor Alan Weinstein, LIGO, and the NSF for making this possible.